Structural Engineering and Mechanics, Vol. 23, No. 4 (2006) 339-352
DOI: http://dx.doi.org/10.12989/sem.2006.23.4.339

Buckling and postbuckling behavior of solid superelastic shape memory alloy shafts

Muhammad Ashiqur Rahman†

Department of Mechanical Engineering, Bangladesh University of Engineering & Technology, Dhaka 1000, Bangladesh

Jinhao Qiu‡ and Junji Tani‡

Institute of Fluid Science, Tohoku University, 2-1-1 Katahira, Sendai 980-8577, Japan

(Received February 24, 2005, Accepted March 15, 2006)

Abstract. Observing the unique stress-strain curves of the superelastic shape memory alloy (SMA) in tension and compression, the primary intention of this study is to investigate the behavior of the shafts made of the same material, under torsional loading-unloading cycles for large angle of twist. Experiments have been performed for the superelastic SMA shafts with different unsupported lengths and angles of twist and the results are compared with those of stainless steel (SUS304) shafts under similar test conditions. As expected for the superelastic SMA, the residual strains are small enough after each cycle and consequently, the hysteresis under loading-reverse loading is much narrower than that for the SUS304. For large angle of twists, the torsional strength of the superelastic SMA increases nonlinearly and exceeds that of SUS304. Most interestingly, the slender solid superelastic SMA shafts are found to buckle when acted upon torsion for large angle of twist.

Keywords: SMA; stress induced martensite; shape recovery; nonlinear stress-strain relations; torsional buckling.

1. Introduction

Torsional buckling can be an important study for the superelastic shape memory alloy (SMA) shafts that exhibits highly nonlinear stress-strain relations. Because of the unique property of superelasticity that depends on the stress induced martensitic transformation (SIMT), superelastic SMA can fully recover large deformation upon withdrawal of the applied load. Consequently, termed as a unique functional material it is extensively used for medical appliances, telephone antenna, head-band for head phones as pointed out by Otsuka and Wayman (1998). That this excellent functional material can exhibit unique mechanical behavior under different loading conditions can be verified from the literature, some of which are listed in the references. For example, Tobushi *et al*. (2000) and later Rahman (2001) and Rahman and Tani (2006) demonstrated

† Associate Professor, Corresponding author, E-mail: ashiq@me.buet.ac.bd
‡ Professor

that the local strain is significantly different from the overall strain during SIMT for an SMA wire under tension. Recently, Rahman and Khan (2006) demonstrated through stress relaxation tests that the so called inertia driven SIMT occurs as local strain increases significantly at constant overall deformation.

Rejnar *et al.* (2002) and Raniecki *et al.* (2000) dealt with the bending of superelastic SMA beams while Rahman *et al.* (2000a, 2000b, 2001, 2005) pointed out the unique buckling characteristics of the superelastic SMA columns. For example, extensively demonstrated through experiment and numerical simulation that columns made of superelastic SMA have unique properties that are completely absent in the columns made of other engineering materials like stainless steel and Al (Rahman *et al.* 2000a, 2000b, 2001, 2005).

The present study, however, concentrates on the experimental demonstration of torsional behavior of the superelastic SMA particularly for large angle of twist. Studying the response of the superelastic SMA under torsional loading will be practically useful and necessary since it has been proposed and used in many practical applications. So far numerous studies have been performed regarding the tensile behavior of the SMA. Only a few studies some of which are listed in the references dealt with the behavior of the SMA under compression, torsion and/or combined loading.

The effect of training on the two-way shape memory (TWSM) for the Cu based polycrystalline SMA under combined loading (torsion and axial load), has been studied by Tokuda *et al.* (2000, 1995) and Sittner *et al.* (1995). The maximum strain during the test was within 2% and the training behavior was demonstrated, related with shape memory effect (SME).

Tanaka *et al.* (1999a) studied the austenitic and martensitic start conditions in a Fe-based polycrystalline SMA under tension/compression-torsion loads. It was demonstrated that an oval cone in the stress-temperature space could represent the martensite start condition while a polygonal cone in the same stress-temperature space could represent the austenite start condition.

Raniecki *et al.* (1999) studied the deformation behavior of TiNi shape memory alloy undergoing R-phase reorientation in torsion-tension (compression) tests. The maximum strain was within 0.5% and the deformation behavior associated with the R-phase reorientation was studied.

Tubular specimens were used for experiments in the above mentioned studies. Besides these studies, Tobushi and Tanaka (1991) developed a model using a simplified torsional stress-strain diagram, for the shape memory alloy spring to represent the load-deflection relation.

As far as the perfect applications of the TWSM training, or other proposed theories related to SME are concerned, the strain in the SMA may remain within a small value (within 2% in most of the above mentioned studies). From mechanical engineering point of view, however, in practical applications the strain can be much larger, in particular, if the shaft material is superelastic SMA. In this respect, Fig. 1 shows the distribution of stresses over the shaft cross-section when acted upon by torsional loading. Because of nonlinearity involved for the stress-strain curve for the SMA, the core of the shaft will be austenitic as shown in the Fig. 1, while beyond this core the shaft material will be in the stress induced martensitic transformation region (slight martensite may also form if the strain is very large).

Besides non-uniform stress distribution over the cross section of an SMA shaft, another important feature is superelastic SMA's asymmetric behavior in tension and compression as reported by Orgeas and Favier (1995), Raniecki and Lexcellent (1998), Rahman *et al.* (2000a, 2000b, 2001). It can be also seen from Fig. 2, the highly nonlinear stress-strain curves of the superelastic SMA in tension and compression exhibit notable asymmetry together with significantly high strength (even higher than that for SUS304) for large strains. Since pure torsion causes both tension and

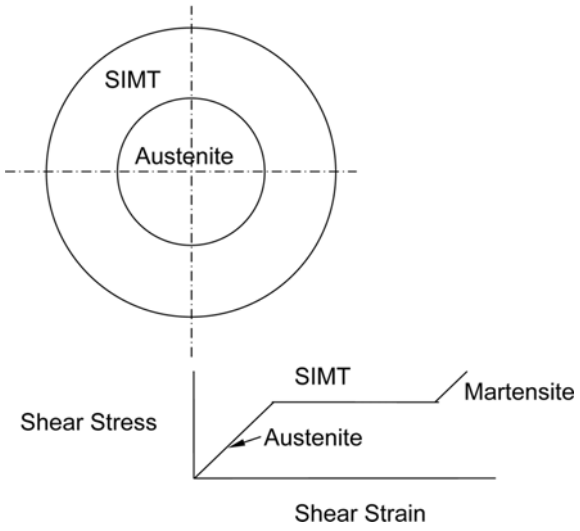

Fig. 1 Stress distribution inside the superelastic SMA shaft

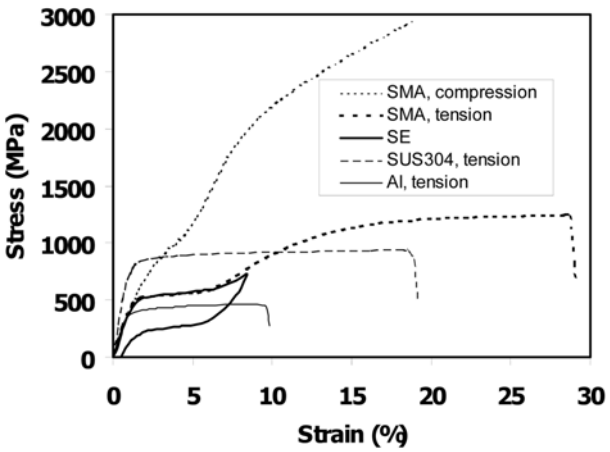

Fig. 2 Nominal stress-strain curves for the SMA, SUS304 and Al

compression of equal magnitude to the stressed element, it is perhaps important to study SMA's behavior under torsion for large angle of twist.

It is important to note that, the true stress strain curves in tension and compression is asymmetric also for the SUS304 columns. But, the asymmetry is much more prominent for the SMA columns as pointed out by Rahman *et al.* (2005, 2006).

Next, torsional buckling of a solid shaft should be discussed from mathematical point of view. Buckling of a solid shaft simply because of torsion is hardly investigated presumably because of the fact that traditionally shafts made of common engineering materials are prone to material failure due to excessive stresses rather than instability failure. Theoretically, however, a solid shaft may also fail due to buckling (Ziegler 1968). As an example, the shaft of Fig. 3, acted upon by a torque M and supported (fixed ends) in the manner of an Euler column, can be investigated.

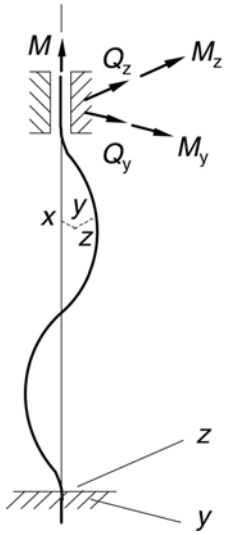

Fig. 3 Buckling of a shaft under pure torsion (after Ziegler 1968)

Since buckling is characterized by a deflection of the initially straight axis, for the present the compliance of the shaft with respect to compression and torsion, together with the influence of shear can be ignored. As long as the axis is straight, the bending moment is zero as in the case of Euler buckling. However, as soon as deflections occur, there appear bending moments in the various sections of the shaft. When they become sufficiently strong, they may result in buckling. For shafts with both ends fixed, mathematical calculation gives the critical twisting moment to be $2.861\pi EI/L$, where, EI is the least flexural rigidity of the shaft (Ziegler 1968). This formulation is on the assumptions similar to those for an ideal Euler column (that is, for linearly elastic materials, ignoring any kind of geometric and physical imperfections).

It was demonstrated in the previous studies of Rahman *et al.* (2000a, 2000b, 2001) that having the unique stress-strain curves (as shown in Fig. 2), columns made of superelastic SMA can exhibit unique buckling and postbuckling characteristics. Therefore, besides the unique capability of superelasticity a superelastic SMA shaft may also exhibit interesting buckling phenomena under pure torsion. To the authors' knowledge rarely any attention has been given so far considering the above mentioned fact. Though a few studies as listed in the references are reported on the torsional behavior of the SMA, none of those concerns buckling. With this perspective, extensive experiments under torsion have been performed in this study for the shafts made of superelastic SMA, and the results are compared with those of SUS304 under similar test conditions.

2. Experiment

2.1 Test conditions

The materials, configurations and conditions used in this experiment are as follows. The chemical composition for the 2 mm solid superelastic SMA rods is Ti49.3 at% Ni50.2at% V0.5at%. The transformation temperatures provided by the manufacturer (Tokin Corporation, Japan) are shown in

Table 1 Transformation temperatures for the SMA (Ti49.3 at% Ni50.2at% V0.5at%)

Transformation temperatures			
Martensite finish (M_f)	Martensite start (M_s)	Austenite start (A_s)	Austenite finish (A_f)
–59°C	–34°C	–27°C	–3°C

Table 1. For comparison of the torsional behavior, 2 mm diameter solid stainless steel (SUS304) rods were also used. The corresponding stress-strain curves (Fig. 2) have been measured from rigorous tests. The Young's modulii (E) are found to be 65 GPA and 210 GPa for the above-mentioned superelastic SMA and SUS304 rods, respectively. The Young's modulus value of SMA, of course, corresponds to the austenite phase.

Test temperature range was 23°C-26°C. The Instron machine was used and the speed during loading-unloading cycle was 1 rpm. For the 2 mm rods, reverse loading for consecutive cycles was performed for a short shaft (L = 40 mm, that is, the slenderness ratio is 80). That shaft was chosen to demonstrate the response of SMA under torsion without any bending or buckling behavior because its slenderness ratio is relatively small. While, loading-unloading cycles were performed and the important buckling behavior of the SMA shafts was examined for L = 80-165 mm, the corresponding slenderness ratio is very high, that is, 160-330.

2.2 Procedure

For the present study involving large angle of twist, avoiding slip of the specimen at the gripping fixtures during the tests was the first task to tackle. Mainly because of slip the test data show high residual strains at the end of loading-unloading cycle. There might be slight plastic deformation as well to cause such residual strains particularly for shafts made of conventional materials. It should be noted here that the term residual strain is used in this study to refer to the angle of twist at the end of loading-unloading cycle when the torque becomes zero. Though it does not rigorously represent the true residual strain of the shaft material, it can, to some extent, evaluate the over all shape recovery capability of the shaft. As mentioned, the specimens were prepared from 2 mm solid rods. To clamp the specimens rigidly in the gripping fixtures, suitable shaped or larger diameter superelastic SMA specimens are expected, which are not available commercially. While dealing with SMA specimens Tanaka *et al.* (1999b) also pointed out the fact that often preparation for a suitable sized SMA specimen, which fits the tests under the loading conditions and exhibits a stable response under repeated loading, is a difficult issue to solve before starting the experiment. For the present study, it becomes very difficult to avoid slip at the gripping fixture when the torque becomes sufficiently large. In order to minimize the occurrence of slip during the tests, two ends of the solid rods were given the suitable shapes by grinding.

Next, it was necessary to find a suitable test method to determine the torsional buckling load of the superelastic SMA shafts. Since torsional buckling is concerned, it is quite difficult to continuously trace the load-transverse deflection curve for an element on the shaft and find the buckling load from those curves. Methods involving the sample moving out of plane and shorting against a tube, were found practically useless in this case. It is because an element on the shaft rotates continuously and at the same time may move in any direction as soon as instability starts. Therefore, the following approach was used in this study to mainly demonstrate and also to find the

shaft's experimental buckling load.

Theoretical buckling loads for the shafts (that is, $2.861\pi E I/L$) were calculated before the tests. Snaps were taken by a digital camera at different states of loading (below and above the theoretically calculated critical twisting moments) to demonstrate that the shape of the deformed SMA shafts changes notably in the vicinity of the theoretical buckling loads.

At this point, it should be noted that the subject matter of this study is to demonstrate experimentally the fact that because of its remarkable high strength at large angle of twist the superelastic SMA shaft buckle unlike the SUS304 shafts. Therefore, the theoretical buckling load was calculated using the original Young's modulus (not the reduced modulus) for all the shafts for the sake of simplicity, and it was shown through pictures taken from a digital camera that the shafts really buckle in the vicinity of this theoretical value. For this, as it would be discussed soon, a load higher than the theoretical one was necessary to clearly demonstrate the buckled shape of the shafts. This adopted method was found to be simple but effective as far as practical demonstration is concerned and can be verified from the subsequent discussions. It would be relevant here to mention that use of digital camera is extensive in measurement of SMA rods. For example, to quantitatively measure strains of an SMA wire Tobushi *et al.* (2000) took help of the digital camera.

3. Results and discussions

Behavior of the 2 mm diameter solid shafts with relatively short test lengths under loading-reverse loading cycles are discussed in the subsection 3.1. For clarity of explanation, buckling and postbuckling behavior of the slender superelastic SMA shafts are dealt exclusively for 2 mm diameter solid shafts in the subsection 3.2.

3.1 Hysteresis for loading-reverse loading cycles

The Instron machine can reverse the direction of torque after the predetermined angle of twist is reached for the loaded shaft. Taking that advantage several loading-reverse loading cycles were obtained for the two shafts as shown in Fig. 4. Fig. 4 presents comparative behavior of the SMA and SUS304 shafts under loading-reverse loading for a few cycles for L = 40 mm. In this study

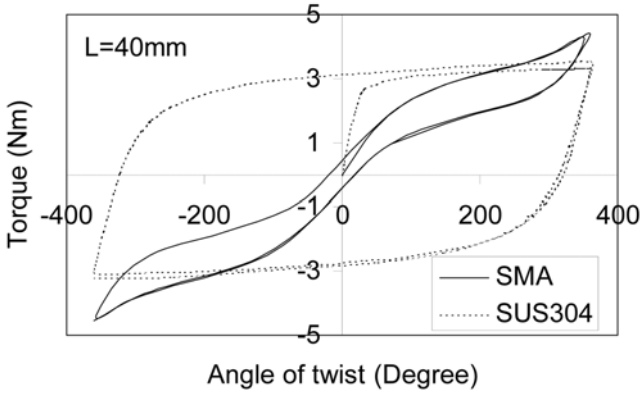

Fig. 4 Hysteresis for the loading-reverse loading cycles under torsion (L = 40 mm)

often torque-angle of twist relations are frequently discussed. This angle of twist is certainly related to the shear strains in the shaft material. Thus, an evaluation of the maximum shear strain on the surface of the shafts could be useful. For 2 mm diameter shafts, using the formula $\gamma = \tan^{-1}(\rho\theta/L)$, the maximum strains on the surface of the rods (ρ = radius) for one complete revolution (θ = 360 degree) are as follows: γ = 15.5% for L = 40 mm and only 3.8% for L = 165 mm.

As can be seen, behavior of both the SMA and SUS304 shafts are almost symmetric for the maximum angle of twist varying from +1 revolution to –1 revolution (Fig. 4). For the SMA shafts, however, the residual strain is very small because of superelasticity and thus the hysteresis is narrow. The SUS304 shaft, on the other hand, deforms plastically and consumes much more amount of energy in comparison with the SMA shaft. Importantly, it is noteworthy that SMA's torsional strength increases nonlinearly and exceeds that of the SUS304 for large angle of twist (Fig. 4).

3.2 Torsional buckling of the slender SMA shafts

Since this study deals with buckling of the shafts, it is necessary to discuss the measures taken to ensure accuracy of the data presented. In this regard, it can be said that both the torque and rotation data are of high resolutions. While recording the data the scales of units can be set at different values. Only to give the idea of accuracy of the data presented in this study, using the Instron machine the rotation (angle of twist) can be measured in degrees up to 3 decimal places. While, the torque, which is more important, was measured by the calibrated load cell in Nm up to 5 decimal places. Though the data are of high resolution, they are presented in round up figures in this study.

Again the buckling phenomenon is imperfection sensitive. Regarding these imperfections, it should be mentioned here that before the shafts were inserted in between the two fixtures, the alignment of the fixtures of the Instron machine, which is highly accurate and reliable, was again checked. It is therefore ensured that the shaft's buckling is not because of any misalignment of the machine's fixtures. Moreover, since perfectly straight slender specimens are practically impossible to manufacture, buckling was observed for at least three different specimens of the same slenderness ratio. Furthermore, the grip slippage was practically eliminated with the ground shapes of the specimens' two ends, as already mentioned. This slippage, if any, would not affect the buckling load's magnitude since it is simultaneously observed and recorded by the digital camera.

As discussed, the torsional stiffness of the SMA increases nonlinearly with the increasing angle of twist. Consequently, it was found from the present study that the slender SMA shafts buckle when the critical twisting moment is exceeded. Upon unloading, however, the shape is recovered due to superelasticity and the shafts again become straight.

As far as the results for buckling and postbuckling behavior for the SMA shaft with L = 140 mm are concerned, the theoretical critical torque is found to be 3.28 Nm. To identify the buckled shapes and the corresponding loads clearly, this shaft was loaded up to 4 Nm and then unloaded. Figs. 5 present the snaps taken at different states of loading. Fig. 5(a) shows the straight configuration of the shaft at 0 Nm. The shaft is slightly deformed at 3.3 Nm (Fig. 5(b)) as the mid-portion becomes convex upward symmetrically. Fig. 5(c) shows the buckled shape of the shaft at 3.4 Nm resembling a sinusoidal profile. To make sure of the fact that the shaft has really buckled at a torque near the theoretical load, the torque was further increased and the distinct buckled shapes can be observed from Figs. 5(d) and 5(e). On the other hand, for L = 140 mm, Figs. 6 show the shapes of the SUS304 shaft corresponding to 0 Nm and 4 Nm. As seen no trace of bending deformation can be observed from Fig. 6(b). In comparison, having much lower Young's modulus, the corresponding

Fig. 5(a) Shape at 0 Nm (SMA shaft, L = 140 mm)

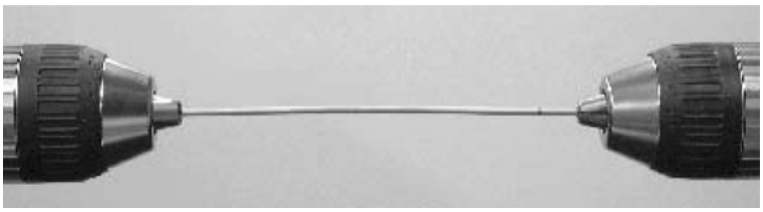

Fig. 5(b) Deformed shape at 3.3 Nm (SMA shaft, L = 140 mm)

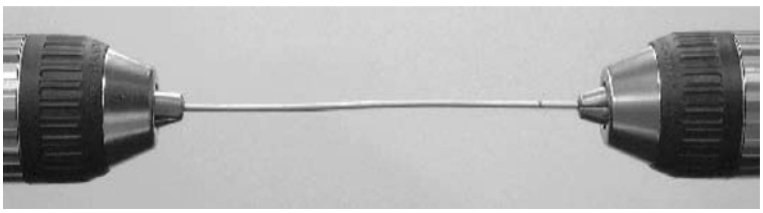

Fig. 5(c) Buckled shape at 3.4 Nm (SMA shaft, L = 140 mm)

Fig. 5(d) Buckled shape at 3.65 Nm (SMA shaft, L = 140 mm)

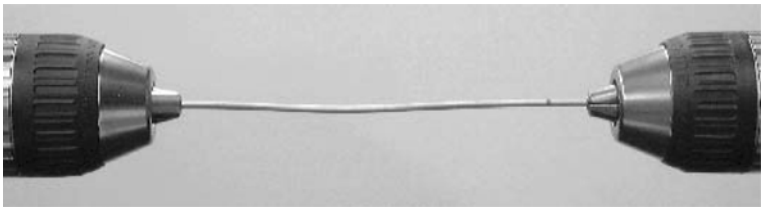

Fig. 5(e) Buckled shape at 4 Nm (SMA shaft, L = 140 mm)

SMA shaft is buckled much below 4 Nm (Figs. 5).

The corresponding torque-angle of twist curve can be observed from Fig. 7. Typically, the superelastic SMA shaft can be twisted far beyond the critical value for buckling. After unloading,

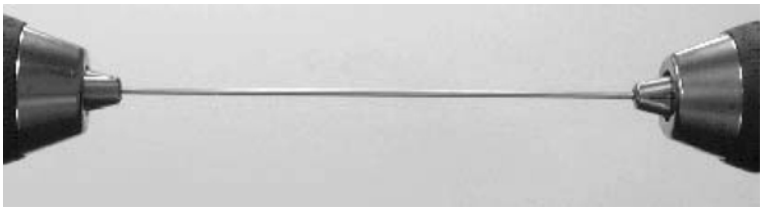

Fig. 6(a) Undeformed shape at 0 Nm (SUS304 shaft, L = 140 mm)

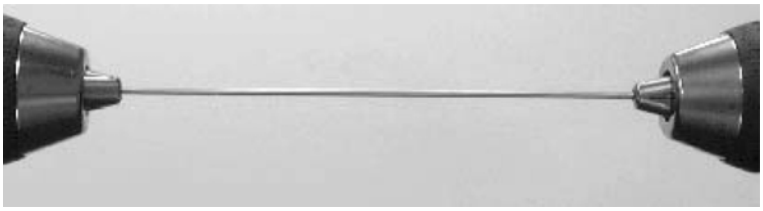

Fig. 6(b) Unbuckled Straight shape at 4 Nm (SUS304 shaft, L = 140 mm)

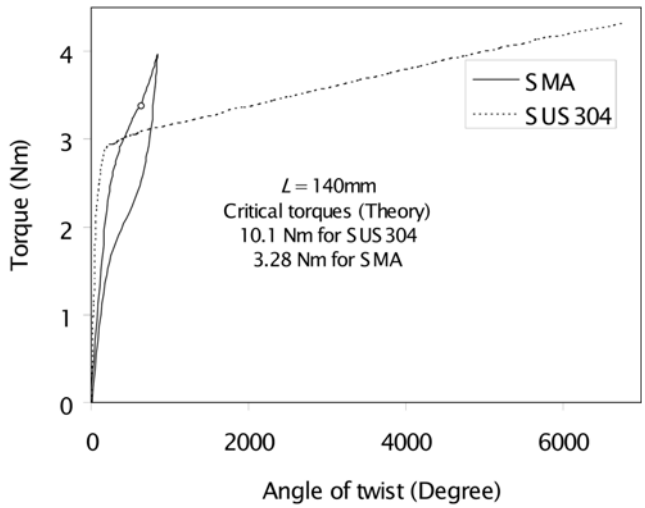

Fig. 7 Load-angle of twist curve for the SMA and SUS304 shafts (L = 140 mm); critical torque, corresponding to buckling, is marked by the circle.

the residual strain is very small for this shaft, indicating it becomes almost straight upon unloading and can be cycled for a number of times to exhibit similar behavior. For the SUS304 shaft, however, the torque increases quite insignificantly for increasing angle of twist. For this shaft the buckling load is 10.1 Nm and therefore large angle of twist is required to reach such a high torque. Thus, usually the material fails before such a high torque (corresponding to the torsional buckling) could be reached.

Typically, SMA's torsional strength increases nonlinearly and exceeds the critical twisting moment with increasing angle of twist. While, for SUS304 shaft with the same value of unsupported length, torque remains almost constant even after large angle of twist. That is the main reason why a

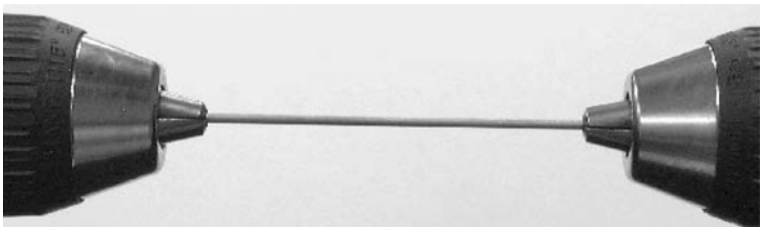

Fig. 8(a) Shape at 0 Nm (SMA shaft, L = 80 mm)

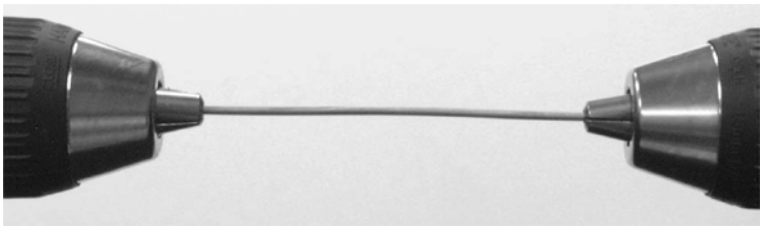

Fig. 8(b) Deformed shape at 4.5 Nm (SMA shaft, L = 80 mm)

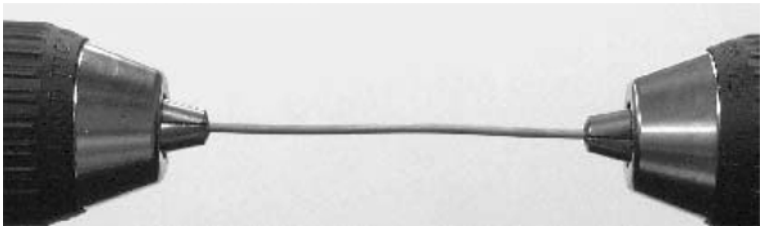

Fig. 8(c) Buckled shape at 5.9 Nm (SMA shaft, L = 80 mm)

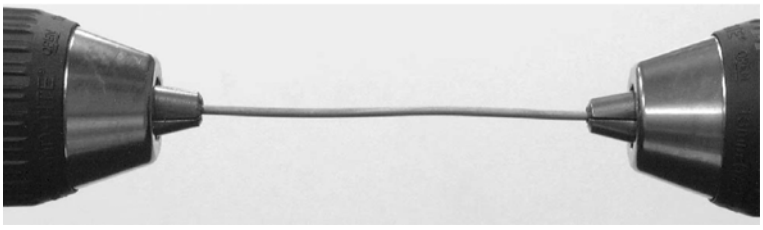

Fig. 8(d) Buckled shape at 6.1 Nm (SMA shaft, L = 80 mm)

slender SMA shaft buckles unlike a SUS304 shaft.

Similarly, the torsional buckling for another shaft of L = 80 mm can also be verified from Figs. 8. The theoretical critical twisting moment is 5.74 Nm. As seen it is distinctly buckled near the vicinity of this value of load (Figs. 8(a)-8(d)). The corresponding torque-angle of twist characteristics can be observed from Fig. 9. Similar to Fig. 7, Fig. 9 also bears the evidence of the fact that typically, SMA's torsional strength increases nonlinearly and exceeds the critical twisting moment with increasing angle of twist. Furthermore, this superelastic SMA shaft can be twisted far beyond the critical value for buckling.

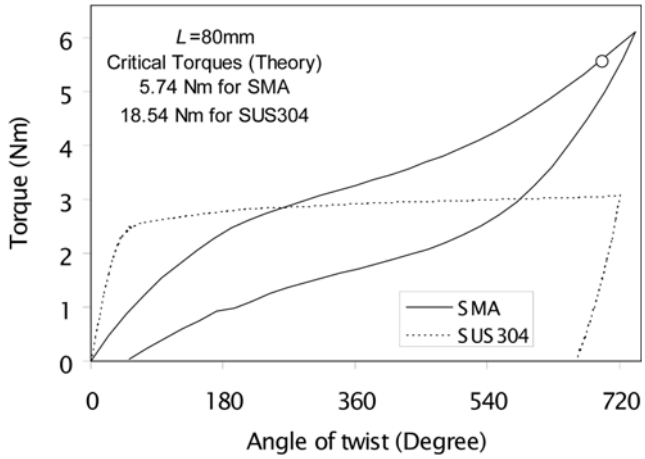

Fig. 9 Load-angle of twist curve for the SMA and SUS304 shafts (L = 80 mm); critical torque, corresponding to buckling, is marked by the circle.

Table 2 Critical twisting moments observed from experiment

	Critical twisting moment (N.m) for the 2 mm superelastic SMA shafts	
L (mm)	Theory	Experiment
165	2.78	Distinct buckled shape observed at 2.9
140	3.28	Distinct buckled shape observed at 3.4
120	3.82	Distinct buckled shape observed at 3.9
100	4.59	Distinct buckled shape observed at 4.9
80	5.74	Distinct buckled shape observed at 5.9

Table 2 gives a comparison of theoretically calculated twisting moments for the shafts, with those experimentally observed. Of course, owing to the unavoidable geometric and physical imperfections, the shafts are likely to buckle at a load lower than the calculated values. However, it should be noted that the critical twisting moment was observed from the pictures of the deformed SMA shafts taken at different states of loading. Since the determination of the buckled shape depends on the eye observation, it is very difficult to determine whether the shaft has prominently changed its shape exactly at the theoretically calculated twisting moment. Thus, to clearly demonstrate the buckled configuration, the load was slightly increased (Table 2) above the calculated critical value and the picture was taken at that state. The question of over prediction of the critical twisting moment should not arise in this context since it is stated more than once that the shaft's buckled shape is presented slightly above the theoretical load only for clear visualization.

It should be noted that tests were performed with at least three different samples for each unsupported length (L) to confirm the figures mentioned in the third column of Table 2. As seen those SMA shafts buckle in the vicinity of the theoretically calculated values.

It has been mentioned here that the critical twisting moments for the other SMA shafts were determined in similar fashion but all results are not presented in order to minimize the number of figures. Interested readers may refer to Rahman (2001) for more details of those results. It can be

concluded that because of unusually steep torque-angle of twist relation, the critical twisting moment is reached for increasing angle of twist and the slender superelastic SMA shafts buckle. If ordinary SMA (with SME) shafts have similar torque-angle of twist relation, they are also likely to buckle under torsion.

In this study comparisons are presented between the torsional behavior of the two types of shafts made of SMA and SUS304 specimens. Steel is the most widely used structural material. That is why, SUS304 has been chosen in this study for comparison purpose where the main topic is the torsional buckling of the slender superelastic SMA shafts. Usually, common steels have similar work hardening response as that of SUS304 as shown in Figs. 4, 7 and 9. Moreover, steel has the highest elastic stiffness among the common engineering materials. Thus, any slender steel shaft's torsional buckling load will also be the highest. If a particular shaft is made of any conventional engineering material that has unusually strong work hardening response, theoretically it may also buckle under twisting moment alike the SMA shaft. But practically, it is more likely that the material itself will break before reaching such a high torque. Furthermore, even if the material does not fail, unlike the superelastic SMA, it will definitely incur extremely large plastic deformations upon unloading and therefore would become practically useless. Rigorous experimental results, as presented in Figs. 7 and 9, can be referred to in support of the above mentioned facts.

Before completing the present discussions, some clarifications should be made regarding the effect of change in room temperature on the superelastic SMA shaft's buckling behavior. Obviously, at extremely high temperatures material may even become soft and at extremely low temperatures superelasticity is not possible at all. That is, at temperatures, abnormally higher or lower than the practically possible room temperatures, certainly, Nitinol superelastic SMA may show all different characteristics which is not the subject matter of this study. In all practical applications superelasticity is utilized at room temperatures and, of course, fixing the transition temperatures through rigorous thermo mechanical treatments, the superelastic SMAs are made solely for that purpose. Interested readers may refer to the works of (Otsuka and Wayman 1998, Tobushi *et al.* 2000) to verify the above mentioned facts. Moreover, all known Nitinol SMAs exhibit more or less similar nonlinear stress-strain behavior as presented in this study (Orgeas and Favier 1995, Raniecki and Lexcellent 1998). Therefore, shafts made of other Nitinol superelastic SMA are likely to show similar torsional buckling behavior at high twisting angle. Slight variation in room temperature is not likely to yield any significant change in the results presented in this study. In this point interested readers may refer to (Rahman *et al.* 2001) where it was comprehensively demonstrated by experimental results that small temperature variation does not at all affect the buckling and postbuckling behavior of the superelastic SMA columns made of the same material as used in this experimental study.

4. Conclusions

A few important characteristics of the solid superelastic SMA shafts have been demonstrated through experimental results. It is found that, if the angle of twist is not very large, the superelastic SMA shafts make a much narrower hysteresis than that of the SUS304 shafts under loading-reverse loading cycles because of small residual strain. Because of superelastic SMA's high strength for large strains, for the increasing angle of twist, its torsional strength increases nonlinearly and exceeds that of the SUS304. As a result, under pure torsion the slender SMA shafts are found to

buckle when the critical twisting moment is exceeded. Examinations of the pictures of the deformed shaft at different state of loading shows that those shafts buckle in the vicinity of the theoretically calculated critical twisting moment. Upon unloading, however, the shape is recovered due to superelasticity and the shafts become straight again. On the other hand, having much higher Young's modulus, the critical twisting moment for the slender SUS304 shaft is about thrice than that for a slender superelastic SMA shaft. Torque-angle of twist curve shows that after the initial portion, the load increases quite insignificantly for increasing angle of twist for the SUS304 shafts. Therefore, in the usual cases of applications the material fails before such a high torque (corresponding to the torsional buckling) is reached. Any trace of bent shape could not be observed examining the pictures of the highly twisted slender SUS304 shaft. Thus, it can be concluded that because of unusually steep torque-angle of twist relation, the slender superelastic SMA shafts buckle for increasing value of the angle of twist. Therefore, care should be taken for the appliances that use superelastic SMA under torsion for sufficiently large angle of twist.

References

Orgeas, L. and Favier, D. (1995), "Non-symmetric tension-compression behaviour of NiTi alloy", *Journal de Physique* IV, Colloque (France) 5 (c8, pt.2), 605-610.

Otsuka, K. and Wayman, C.M. (1998), *Shape Memory Materials*, Cambridge University Press.

Rahman, M.A. (2001), "Behavior of the superelastic shape memory alloy columns under compression and torsion", Ph D Thesis, Tohoku University, Japan.

Rahman, M.A. and Khan, R.M. (2006), "Unique local deformations of the superelastic SMA rods during stress-relaxation tests", *Struct. Eng. Mech., Int. J.,* **22**(5), 563-574.

Rahman, M.A. and Tani, J. (2006), "Local deformation characteristics of the shape memory alloy rods during forward and reverse stress induced martensitic transformations", *J. Intelligent Material Systems and Structures* (In Press).

Rahman, M.A., Qiu, J. and Tani, J. (2000), "Behaviors of the short superelastic SMA columns under compressive loading-unloading cycles", *Proc. of the JSME Tohoku Branch Conf.* (in Japanese), 67-68.

Rahman, M.A., Qiu, J. and Tani, J. (2000), "Behaviors of the superelastic SMA columns under compressive loading-unloading cycles", *Proc. of the 11th Int. Conf. on Adaptive Structures and Technology* (Nagoya, Japan), 351-358.

Rahman, M.A., Qiu, J. and Tani, J. (2001), "Buckling and postbuckling characteristics of the superelastic SMA columns", *Int. J. Solids Struct.,* **38**, 9253-9265.

Rahman, M.A., Qiu, J. and Tani, J. (2005), "Buckling and postbuckling characteristics of the superelastic SMA columns-Numerical Simulation", *J. Intelligent Material Systems and Structures,* **16**(9), 691-702.

Rahman, M.A., Tani, J. and Afsar, A.M. (2006), "Postbuckling behaviour of stainless steel columns under loading-unloading cycles", *J. of Constructional Steel Research* (In Press).

Raniecki, B. and Lexcellent, C.H. (1998), "Thermodynamics of isotropic pseudoelasticity in shape memory alloys", *Eur. J. Mech., A/Solids*, **17**(2), 185-205.

Raniecki, B., Miyazaki, S., Tanaka, K., Dietrich, L. and Lexcellent, C. (1999), "Deformation behavior of TiNi shape memory alloy undergoing R-phase reorientation in torsion-tension (compression) tests", *Arch. Mech.*, **51**(6), 745-784.

Raniecki, B., Rejnar, J. and Lexcellent, C.H. (2001), "Anatomization of hysteresis loops in pure bending of ideal pseudoelastic beams", *Int. J. Mech. Sci.*, **43**(5), 1339-1368.

Rejnar, J., Lexcellent, C. and Raniecki, B. (2002), "Pseudoelastic behaviour of shape memory alloy beams under pure bending; Experiment and modelling", *Int. J. Mech. Sci.,* **44**, 665-686.

Sittner, P., Hara, Y. and Tokuda, M. (1995), "Experimental study on the thermoelastic martensitic transformation in shape memory alloy polycrystal induced by combined external force", *Metallurgical and Materials Transactions A*, **26A**, 2923-2935.

Tanaka, K. and Watanabe, T. (1999), "Transformation conditions in an Fe-based shape memory alloy: An experimental study", *Arch. Mech.*, **51**(6), 805-832.
Tanaka, K., Kitamura, K. and Miyazaki, S. (1999), "Shape memory alloy preparation for multiaxial tests and identification of fundamental alloy performance", *Arch. Mech.*, **51**(6).
Tobushi, H. and Tanaka, K. (1991), "Deformation of a shape memory alloy helical spring (analysis based on stress-strain-temperature relation)", *JSME Int. J.*, series I, **34**(1), 83-89.
Tobusi, H., Okumura, K., Endo, M. and Takata, K. (2000), "Stress-induced martensitic transformation behavior and lateral strain of TiNi shape memory alloy", *Proc. of the 11th ICAST*, 367-374, Nagoya.
Tokuda, M., Sittner, P., Takakura, M. and Ye, M. (1995), "Experimental study on performances in Cu-based shape memory alloy under multi-axial loading conditions", *Mater. Sci. Res. Int.*, **1**(4), 260-265.
Tokuda, M., Sugino, S. and Inaba, T. (2000), "Two-way shape memory behavior obtained by combined loading training", *Proc. of the 11th ICAST* (Nagoya), 382-389.
Ziegler, H. (1968), *Principles of Structural Stability*. Blaisdell publishing company, a division of Ginn and company.